Mott Criticality as the Confinement Transition of a Pseudogap-Mott Metal

Presentation for Postdoctoral Position at ICTS-TIFR

Abhirup Mukherjee

Department of Physical Sciences,
Indian Institute of Science Education and Research Kolkata

January 6, 2026

A Brief Introduction

University of Calcutta **(B.Sc. Physics)** — *2018*

IISER Kolkata **(M.S.)** — *2021*

IISER Kolkata **(Ph.D., Prof. S Lal)** — *2026**

Research Interests

- Mott transition and criticality
- Unconventional superconductivity
- Various forms of quantum matter

Skills and Techniques

- Field theory (RG methods) and effective theory-based techniques
- Numerical computation of correlation functions, entanglement measures, dynamical correlations (spectral function, self-energy, etc)
- Developed new method for using quantum impurity models to analyse interacting lattice models
- Developed Python and Julia libraries

List of Projects

- **Mott Criticality as the Confinement Transition of a Pseudogap-Mott Metal**. arXiv:2507.17201 (2025)
- Revealing the magnetic dimensional crossover in the Heisenberg ferromagnet CrSiTe3 through picosecond strain pulses. Phys. Rev. B 111, L140414 (2025)
- **Holographic entanglement renormalisation for fermionic quantum matter**. J. Phys. A: Math. Theor. 57 275401 (2024)
- **Kondo frustration via charge fluctuations: a route to Mott localisation**. New J. Phys. 25 113011 (2023)
- Frustration shapes multi-channel Kondo physics: a star graph perspective. J. Phys.: Condens. Matter 35 315601 (2023)
- Unveiling the Kondo cloud: Unitary renormalization-group study of the Kondo model. Phys. Rev. B 105, 085119 (2022)

Some Questions

The anomalous **pseudogap** (PG) phase exhibits nodal-antinodal dichotomy.

No general consensus yet regarding

- nature of $T = 0$ ground states of the cuprates
- **relation** of PG to Mott insulating and superconducting phases proximate to it
- how pseudogap **evolves** from weak- to strong-coupling
- nature of correlations and entanglement near the transition

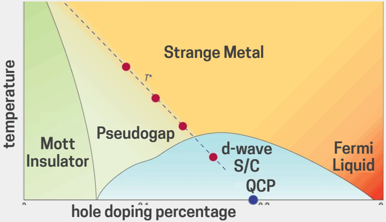

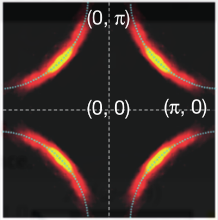

Keimer et al. 2015; Proust and Taillefer 2019; Loeser et al. 1996; Norman et al. 1998; Hashimoto et al. 2014; Kyung et al. 2006; Macridin et al. 2006; Wu et al. 2018; Mukherjee and Lal 2020; Hille et al. 2020.

New Auxiliary Model Approach To Interacting Fermions

1. Solve an **impurity model** H_{imp} with certain properties:
   - Lattice symmetry
   - Impurity phase transition

2. **Construct lattice** model by applying many-body translation operators:

$$H_{\mathrm{latt}} = \sum_{\mathbf{r}} T^{\dagger}(\mathbf{r}) H_{\mathrm{imp}}(\mathbf{r_0}) T(\mathbf{r})$$

3. Relate computables across the models, using many-body Bloch's theorem

Greens functions:

$$\tilde{G}(\mathbf{K}\sigma;\omega) = G^{>}(T^{\dagger}_{\mathbf{K}\sigma}, \omega - \varepsilon_{\mathbf{K}}) + G^{<}(T^{\dagger}_{\mathbf{K}\sigma}, \omega + \varepsilon_{\mathbf{K}})$$

Equal-time **correlation** functions:

$$C_O(\mathbf{k}_1, \mathbf{k}_2) = \sum_{\Delta} \langle \mathbf{r}_c + \Delta | \tilde{O}(\mathbf{k}_2) | \mathbf{r}_c \rangle \langle \mathbf{r}_c | \tilde{O}^{\dagger}(\mathbf{k}_1) | \mathbf{r}_c \rangle$$

where

$$G^{>}(O^{\dagger}, t) = -i \langle O(t) O^{\dagger} \rangle,$$

(imp-bath T-matrix)

$$T_{\mathbf{K}\sigma} = c_{\mathbf{K}\sigma} \left(\textstyle\sum_{\sigma'} c^{\dagger}_{d\sigma} + \text{h.c.} \right) + c_{\mathbf{K}\sigma} \left(S_d^{+} + \text{h.c.} \right),$$

$$\tilde{O}(\mathbf{r}) = O(\mathbf{r}) O^{\dagger}(d)$$

Stoyanova 2006; Maier et al. 2005; Sakai 2023.

The Core Ingredient: A Lattice-Embedded Impurity Model

$$H_{\text{imp}} = H_{\text{2D-TB-KE}} - \frac{U}{2}\left(n_{d\uparrow} - n_{d\downarrow}\right)^2 + V\sum_{Z,\sigma}\left(c^\dagger_{d\sigma}c_{Z\sigma} + \text{h.c.}\right) + J\sum_{Z}\mathbf{S}_d\cdot\mathbf{S}_Z$$
$$- \frac{W}{2}\sum_{Z}\left(n_{Z\uparrow} - n_{Z\downarrow}\right)^2 \quad (1)$$

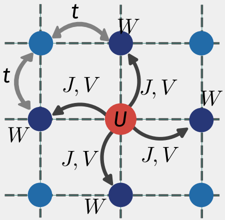

- $J_{\mathbf{k},\mathbf{k}'}$ has C_4**-symmetry**:

$$J_{\mathbf{k},\mathbf{k}'} = \frac{J}{2}\left[\cos\left(\mathbf{k}_x - \mathbf{k}'_x\right) + \cos\left(\mathbf{k}_y - \mathbf{k}'_y\right)\right]$$

The Core Ingredient: A Lattice-Embedded Impurity Model

$$H_{\mathrm{imp}} = H_{\text{2D-TB-KE}} - \frac{U}{2}\left(n_{d\uparrow} - n_{d\downarrow}\right)^2 + V\sum_{Z,\sigma}\left(c^\dagger_{d\sigma}c_{Z\sigma} + \mathrm{h.c.}\right) + J\sum_{Z}\mathbf{S}_d\cdot\mathbf{S}_Z$$
$$- \frac{W}{2}\sum_{Z}\left(n_{Z\uparrow} - n_{Z\downarrow}\right)^2 \qquad (1)$$

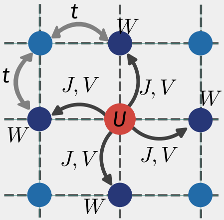

- $J_{\mathbf{k},\mathbf{k}'}$ has C_4**-symmetry**:

$$J_{\mathbf{k},\mathbf{k}'} = \frac{J}{2}\left[\cos\left(\mathbf{k}_x - \mathbf{k}'_x\right) + \cos\left(\mathbf{k}_y - \mathbf{k}'_y\right)\right]$$

Map to Hubbard-Heisenberg Model

$$H_{\mathrm{latt}} = \sum_{\mathbf{r}} T^\dagger(\mathbf{r})H_{\mathrm{imp}}(\mathbf{r_0})T(\mathbf{r})$$
$$= -\frac{\tilde{t}}{\sqrt{Z}}\sum_{\langle \mathbf{r}_i,\mathbf{r}_j\rangle;\sigma}\left(c^\dagger_{\mathbf{r}_i,\sigma}c_{\mathbf{r}_j,\sigma} + \mathrm{h.c.}\right) - \tilde{\mu}\sum_{\mathbf{r}}\hat{n}_{\mathbf{r},\sigma}$$
$$+ \frac{\tilde{J}}{Z}\sum_{\langle \mathbf{r}_i,\mathbf{r}_j\rangle}\mathbf{S}_{\mathbf{r}_i}\cdot\mathbf{S}_{\mathbf{r}_j} - \frac{1}{2}\tilde{U}\sum_{\mathbf{r}}\left(\hat{n}_{\mathbf{r},\uparrow} - \hat{n}_{\mathbf{r},\downarrow}\right)^2$$

$$\tilde{t} = t + 2V$$

$$\tilde{U} = U + W$$

$$\tilde{\mu} = 2\mu + \eta, \quad \tilde{J} = 2J$$

The Core Ingredient: A Lattice-Embedded Impurity Model

$$H_{\mathrm{imp}} = H_{\text{2D-TB-KE}} - \frac{U}{2}\left(n_{d\uparrow} - n_{d\downarrow}\right)^2 + V\sum_{Z,\sigma}\left(c^{\dagger}_{d\sigma}c_{Z\sigma} + \text{h.c.}\right) + J\sum_{Z}\mathbf{S}_d\cdot\mathbf{S}_Z$$
$$- \frac{W}{2}\sum_{Z}\left(n_{Z\uparrow} - n_{Z\downarrow}\right)^2$$

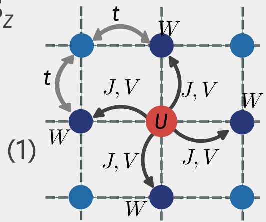

- $J_{\mathbf{k},\mathbf{k}'}$ has C_4**–symmetry**:

$$J_{\mathbf{k},\mathbf{k}'} = \frac{J}{2}\left[\cos\left(\mathbf{k}_x - \mathbf{k}'_x\right) + \cos\left(\mathbf{k}_y - \mathbf{k}'_y\right)\right]$$

Map to Hubbard-Heisenberg Model

$$H_{\mathrm{latt}} = \sum_{\mathbf{r}} T^{\dagger}(\mathbf{r})H_{\mathrm{imp}}(\mathbf{r_0})T(\mathbf{r})$$
$$= -\frac{\tilde{t}}{\sqrt{Z}}\sum_{\langle\mathbf{r}_i,\mathbf{r}_j\rangle;\sigma}\left(c^{\dagger}_{\mathbf{r}_i,\sigma}c_{\mathbf{r}_j,\sigma} + \text{h.c.}\right) - \tilde{\mu}\sum_{\mathbf{r}}\hat{n}_{\mathbf{r},\sigma}$$
$$+ \frac{\tilde{J}}{Z}\sum_{\langle\mathbf{r}_i,\mathbf{r}_j\rangle}\mathbf{S}_{\mathbf{r}_i}\cdot\mathbf{S}_{\mathbf{r}_j} - \frac{1}{2}\tilde{U}\sum_{\mathbf{r}}\left(\hat{n}_{\mathbf{r},\uparrow} - \hat{n}_{\mathbf{r},\downarrow}\right)^2$$

$$\tilde{t} = t + 2V$$
$$\tilde{U} = U + W$$
$$\tilde{\mu} = 2\mu + \eta,\quad \tilde{J} = 2J$$

- We work in large U limit
- SW transformation $\rightarrow$ $J - W$ **model**

Pseudogapping Transition from Kondo Breakdown

Unitary RG analysis - integrate out high-energy states in the conduction bath:

$$\Delta J^{(j)}_{\mathbf{k}_1,\mathbf{k}_2} = -\sum_{\mathbf{q}\in \mathrm{PS}} \frac{J^{(j)}_{\mathbf{k}_2,\mathbf{q}} J^{(j)}_{\mathbf{q},\mathbf{k}_1} + 4 J^{(j)}_{\mathbf{q},\bar{\mathbf{q}}} W_{\bar{\mathbf{q}},\mathbf{k}_2,\mathbf{k}_1,\mathbf{q}}}{\omega - \frac{1}{2}|\varepsilon_j| + J^{(j)}_{\mathbf{q}}/4 + W_{\mathbf{q}}/2}$$

Pseudogapping Transition from Kondo Breakdown

Unitary RG analysis - integrate out high-energy states in the conduction bath:

$$\Delta J^{(j)}_{\mathbf{k}_1,\mathbf{k}_2} = -\sum_{\mathbf{q}\in \mathrm{PS}} \frac{J^{(j)}_{\mathbf{k}_2,\mathbf{q}} J^{(j)}_{\mathbf{q},\mathbf{k}_1} + 4 J^{(j)}_{\mathbf{q},\bar{\mathbf{q}}} W_{\bar{\mathbf{q}},\mathbf{k}_2,\mathbf{k}_1,\mathbf{q}}}{\omega - \frac{1}{2}|\varepsilon_j| + J^{(j)}_{\mathbf{q}}/4 + W_{\mathbf{q}}/2}$$

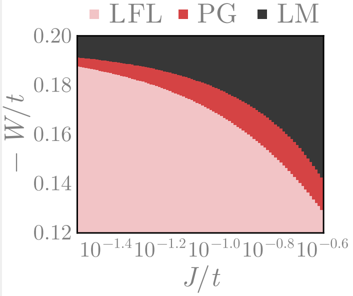

- momentum-**anistropic** screened phase between SC and LM phases.
- Contrast with **eSIAM**: $\Delta J \sim J(J + 4W)$

Pseudogapping Transition from Kondo Breakdown

Unitary RG analysis - integrate out high-energy states in the conduction bath:

$$\Delta J^{(j)}_{\mathbf{k}_1,\mathbf{k}_2} = -\sum_{\mathbf{q}\in \mathrm{PS}} \frac{J^{(j)}_{\mathbf{k}_2,\mathbf{q}} J^{(j)}_{\mathbf{q},\mathbf{k}_1} + 4 J^{(j)}_{\mathbf{q},\bar{\mathbf{q}}} W_{\bar{\mathbf{q}},\mathbf{k}_2,\mathbf{k}_1,\mathbf{q}}}{\omega - \frac{1}{2}|\varepsilon_j| + J^{(j)}_{\mathbf{q}}/4 + W_{\mathbf{q}}/2}$$

- momentum-**anistropic** screened phase between SC and LM phases.
- Contrast with **eSIAM**: $\Delta J \sim J(J + 4W)$
- Impurity-bath spin correlations show k-differentiation

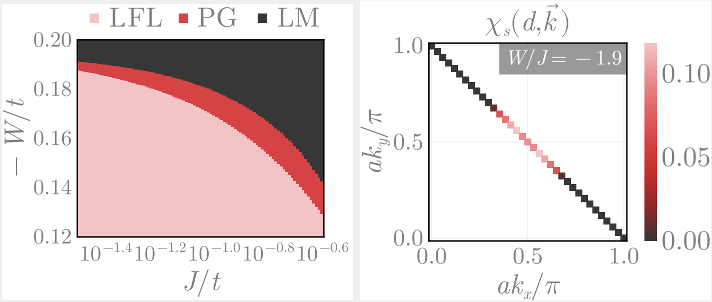

Pseudogapping Transition from Kondo Breakdown

Unitary RG analysis - integrate out high-energy states in the conduction bath:

$$\Delta J^{(j)}_{\mathbf{k}_1,\mathbf{k}_2} = -\sum_{\mathbf{q}\in \mathrm{PS}} \frac{J^{(j)}_{\mathbf{k}_2,\mathbf{q}} J^{(j)}_{\mathbf{q},\mathbf{k}_1} + 4 J^{(j)}_{\mathbf{q},\bar{\mathbf{q}}} W_{\bar{\mathbf{q}},\mathbf{k}_2,\mathbf{k}_1,\mathbf{q}}}{\omega - \frac{1}{2}|\varepsilon_j| + J^{(j)}_{\mathbf{q}}/4 + W_{\mathbf{q}}/2}$$

- momentum-**anistropic** screened phase between SC and LM phases.
- Contrast with **eSIAM**: $\Delta J \sim J(J + 4W)$
- Impurity-bath spin correlations show k–differentiation
- Lattice model DOS shows **P-gap**

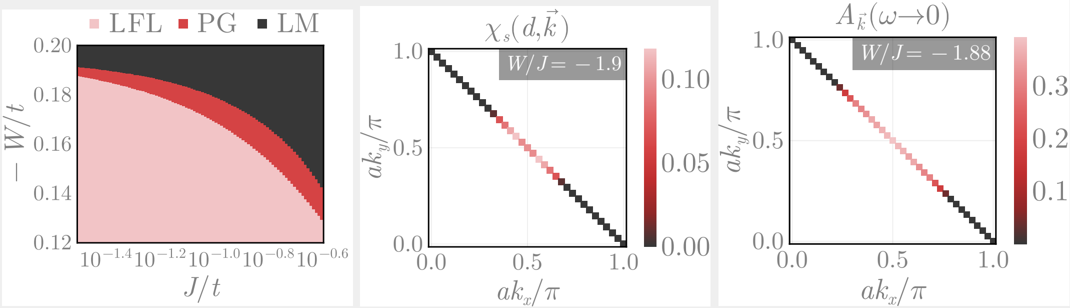

Local Fermi Liquid and Local Moment Phases

LFL

- Democratic screening in k-space, broad $\omega = 0$ **resonance**
- 1-particle excitations → Fermi liquid upon tiling
- $\Sigma'' \sim \omega^2$

These phases also exist in the **eSIAM**.

LM

- Unscreened moment. Spectral function gapped.
- $\Sigma \sim 1/\omega$
- Irrelevant hopping processes lead to Heisenberg model

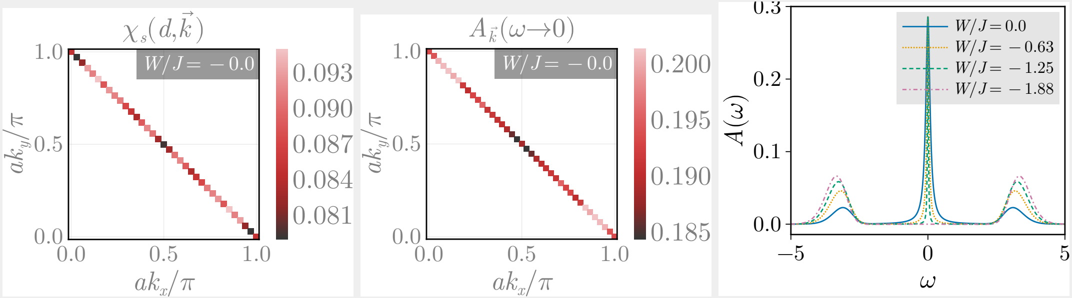

Unravelling of Kondo screening

The Kondo breakdown process can be visualised in terms of **zeros** of $J_{\mathbf{k}_N,\mathbf{k}}$.

- $J_{\mathbf{k}_N,\mathbf{k}}$ for $\mathbf{k}$ close to the **adjacent nodes** turn RG irrelevant first, and a patch of zeros subsequently appears in $J_{\mathbf{k}_N,\mathbf{k}}$ around this point.

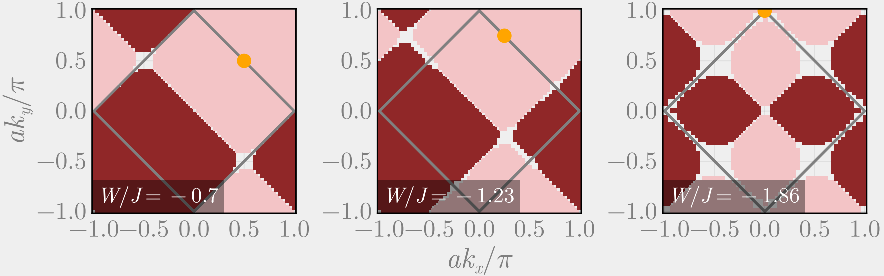

Unravelling of Kondo screening

The Kondo breakdown process can be visualised in terms of **zeros** of $J_{\mathbf{k}_N,\mathbf{k}}$.

- $J_{\mathbf{k}_N,\mathbf{k}}$ for $\mathbf{k}$ close to the **adjacent nodes** turn RG irrelevant first, and a patch of zeros subsequently appears in $J_{\mathbf{k}_N,\mathbf{k}}$ around this point.
- Tuning W/J further extends the patch of zeros in $J_{\mathbf{k}_1,\mathbf{k}_2}$ for all $\mathbf{k}_1$ lying between a given node and the nearest antinodes.

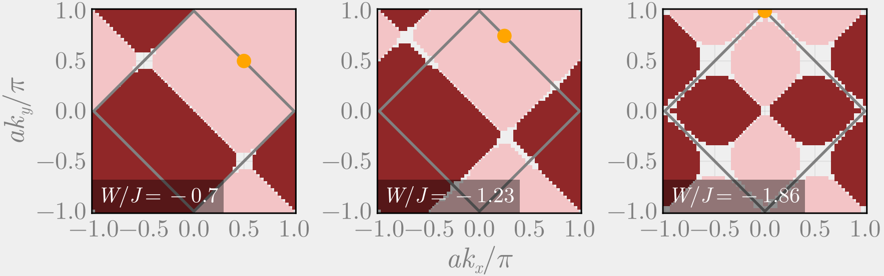

Unravelling of Kondo screening

The Kondo breakdown process can be visualised in terms of **zeros** of $J_{\mathbf{k}_N,\mathbf{k}}$.

- $J_{\mathbf{k}_N,\mathbf{k}}$ for $\mathbf{k}$ close to the **adjacent nodes** turn RG irrelevant first, and a patch of zeros subsequently appears in $J_{\mathbf{k}_N,\mathbf{k}}$ around this point.
- Tuning W/J further extends the patch of zeros in $J_{\mathbf{k}_1,\mathbf{k}_2}$ for all $\mathbf{k}_1$ lying between a given node and the nearest antinodes.
- At $W = W_{PG}$, the **antinode** joins this connected region of zeros in $J_{\mathbf{k}_1,\mathbf{k}_2}$, marking the onset of the PG. The antinode **decouples** from all Fermi points.

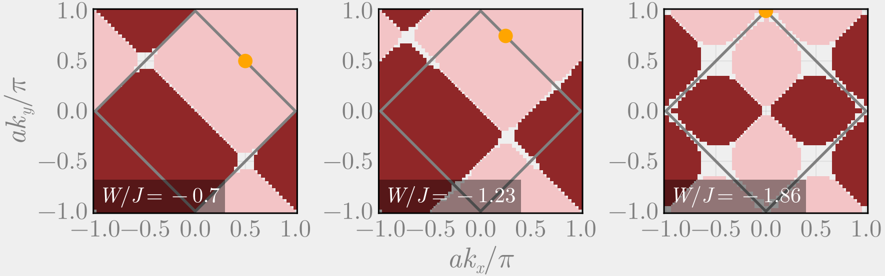

Dynamical Spectral Weight Transfer

- strong fluctuations observed in **charge correlations** between the gapless nodal and gapped antinodal regions in PG regime
- PG results from **selective transfer** of spectral weight from low to high energies
- **Differs from eSIAM** (spectral weight transferred from entire FS at once)
- PG coincides with the appearance of poles of the lattice self-energy $\Sigma(\mathbf{k}, \omega = 0)$ near the antinodes

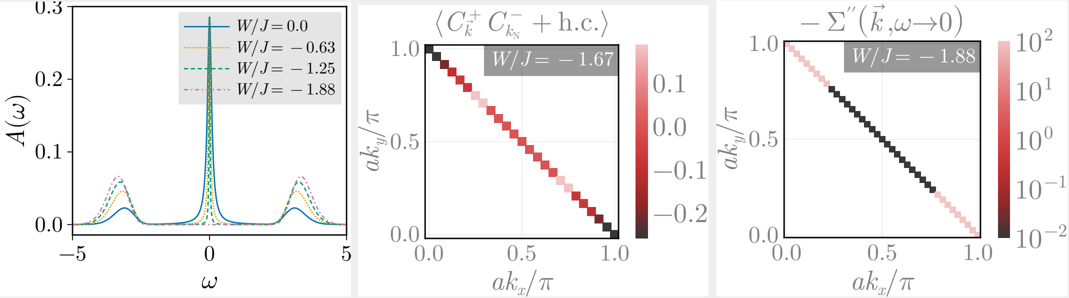

Non-Fermi liquid nature of the pseudogap

Kondo scattering processes can be divided into two classes

- H_{ch1}, H_{ch2}: **Within** the green/pink regions
- H_{1-2}: **Connecting** the green and pink regions
- Fermi liquid: $H_{ch1} = H_{ch2} \simeq H_{1-2}$

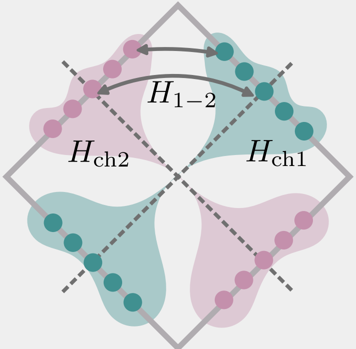

Non-Fermi liquid nature of the pseudogap

Kondo scattering processes can be divided into two classes

- H_{ch1}, H_{ch2}: **Within** the green/pink regions
- H_{1-2}: **Connecting** the green and pink regions
- Fermi liquid: $H_{ch1} = H_{ch2} \simeq H_{1-2}$

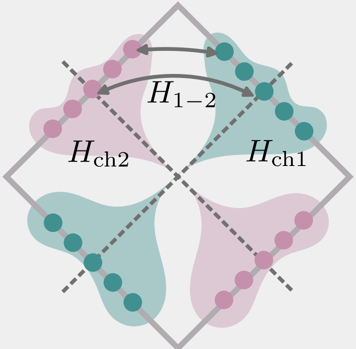

- Pseudogap: H_{1-2} **irrelevant**:

$$H = H_{ch1} + H_{ch2}$$

- Effective **two-channel Kondo** description - each pair of opposite quadrants forms a channel

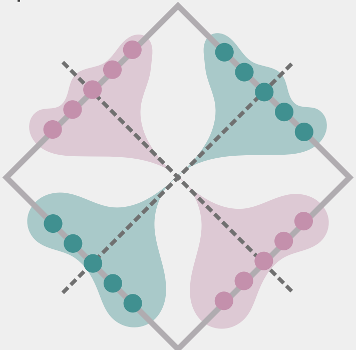

Non-Fermi liquid nature of the pseudogap

2CK guaranteed by **symmetry** of Kondo coupling:

$$|J(k_1, k_2)| = |J(k_1 + \vec{\pi}, k_2)|$$

2CK → **non-Fermi liquid** excitations!

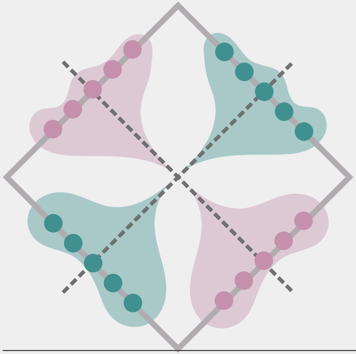

Coleman, Ioffe, and Tsvelik 1995; Schofield 1997; Varma, Nussinov, and Van Saarloos 2002; Patra et al. 2023.

Non-Fermi liquid nature of the pseudogap

2CK guaranteed by **symmetry** of Kondo coupling:

$$|J(k_1, k_2)| = |J(k_1 + \vec{\pi}, k_2)|$$

2CK → **non-Fermi liquid** excitations!

- **Marginal FL** behaviour: $\Sigma' \sim \omega \ln \omega$
- quasiparticle residue, $Z \sim 1/\ln \omega$ (vanishes logarithmically)
- Partially **unscreened** moment

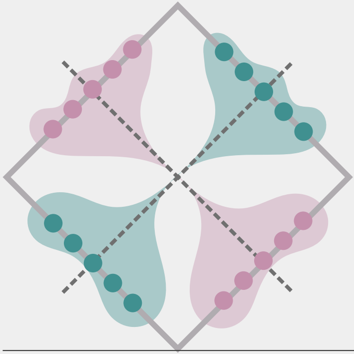

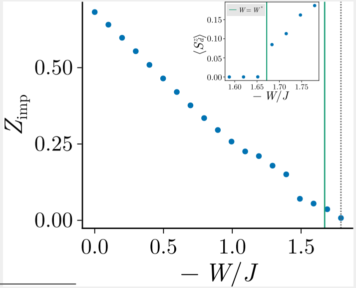

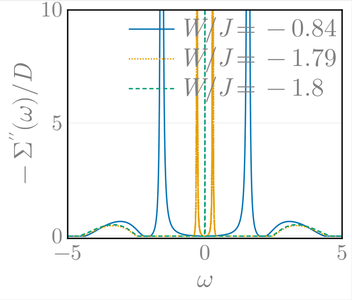

Coleman, Ioffe, and Tsvelik 1995; Schofield 1997; Varma, Nussinov, and Van Saarloos 2002; Patra et al. 2023.

Singular Nodal Metal

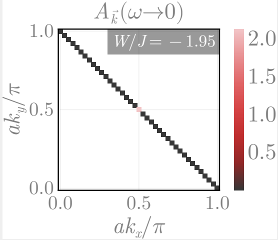

Close to transition, screening concentrated in **nodal regions**

Singular Nodal Metal

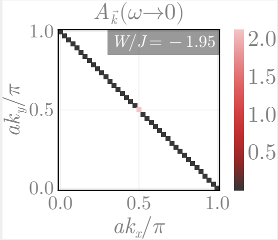

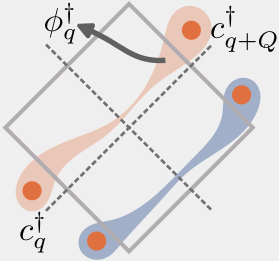

Close to transition, screening concentrated in **nodal regions**

Low-energy excitations:

- Integrate out impurity spin-flips (J^2/W)
- SW transformation → effective Hamiltonian

Emergent modes:

$$\phi_{\mathbf{q},\sigma} = \frac{1}{\sqrt{2}}\left(c_{\mathbf{N}_1+\mathbf{q},\sigma} - c_{\mathbf{N}_1+\mathbf{Q}_1-\mathbf{q},\sigma}\right), \quad r = \phi^\dagger\phi$$

Singular Nodal Metal

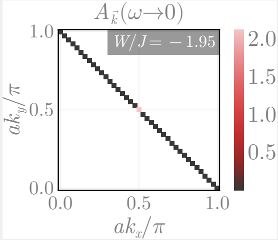

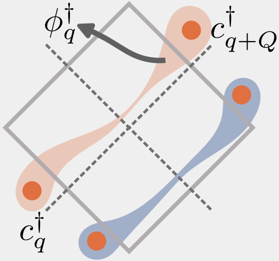

Close to transition, screening concentrated in **nodal regions**

Low-energy excitations:

- Integrate out impurity spin-flips (J^2/W)
- SW transformation → effective Hamiltonian

Emergent modes:

$$\phi_{\mathbf{q},\sigma} = \frac{1}{\sqrt{2}}\left(c_{\mathbf{N}_1+\mathbf{q},\sigma} - c_{\mathbf{N}_1+\mathbf{Q}_1-\mathbf{q},\sigma}\right), \quad r = \phi^\dagger\phi$$

$$\Delta\tilde{H} = \underbrace{\sum_{\mathbf{q},\sigma} \frac{|\varepsilon_{\mathbf{N}_1+\mathbf{q}}|\varepsilon_{\mathbf{N}_1+\mathbf{q}}}{-W} r_{\mathbf{q},\sigma}}_{\text{dispersion}} + \sum_{\mathbf{q}_1,\mathbf{q}_2,\sigma} \frac{J^{*2}}{-4W}\left[\underbrace{r_{\mathbf{q}_1\sigma}\left(1 - r_{\mathbf{q}_2\bar{\sigma}}\right)}_{\text{density interaction}} - (1-\delta_{\mathbf{q}_1,\mathbf{q}_2})\underbrace{\phi^\dagger_{\mathbf{q}_1,\bar{\sigma}}\phi^\dagger_{\mathbf{q}_1,\sigma}\phi_{\mathbf{q}_2,\sigma}\phi_{\mathbf{q}_2,\bar{\sigma}}}_{\text{fwd/tang. pair transfer}}\right]$$

Singular Nodal Metal

We focus on the simplified case of zero momentum transfer $q_1 = q_2$:

$$\Delta\tilde{H} = \sum_{\mathbf{q},\sigma} \epsilon_{\mathbf{q}} r_{\mathbf{q},\sigma} + u \sum_{\mathbf{q},\sigma} r_{\mathbf{q}\sigma} r_{\mathbf{q}\bar{\sigma}}, \quad \phi_{\mathbf{q},\sigma} = \frac{1}{\sqrt{2}}\left(c_{\mathbf{N}_1+\mathbf{q},\sigma} - c_{\mathbf{N}_1+\mathbf{Q}_1-\mathbf{q},\sigma}\right), \ r = \phi^\dagger\phi$$

$$\epsilon_{\mathbf{q}} = \frac{|\varepsilon_{\mathbf{N}_1+\mathbf{q}}|\varepsilon_{\mathbf{N}_1+\mathbf{q}}}{-W} + \frac{J^{*2}}{-4W}, \ u = \frac{J^{*2}}{4W}$$

- Nodal metal is described by a **Hatsugai-Kohmoto model**.
- Non-Fermi liquid excitations.

$$\Sigma \sim \frac{u^2}{\omega}, Z \sim \omega^2$$

Σ pole continues into **Mott insulator**.

Baskaran 1991; Hatsugai and Kohmoto 1992; Phillips, Yeo, and Huang 2020.

Singular Nodal Metal

We focus on the simplified case of zero momentum transfer $q_1 = q_2$:

$$\Delta\tilde{H} = \sum_{\mathbf{q},\sigma} \epsilon_{\mathbf{q}} r_{\mathbf{q},\sigma} + u \sum_{\mathbf{q},\sigma} r_{\mathbf{q}\sigma} r_{\mathbf{q}\bar{\sigma}}, \quad \phi_{\mathbf{q},\sigma} = \frac{1}{\sqrt{2}}\left(c_{\mathbf{N}_1+\mathbf{q},\sigma} - c_{\mathbf{N}_1+\mathbf{Q}_1-\mathbf{q},\sigma}\right), \; r = \phi^\dagger\phi$$

$$\epsilon_{\mathbf{q}} = \frac{|\varepsilon_{\mathbf{N}_1+\mathbf{q}}|\varepsilon_{\mathbf{N}_1+\mathbf{q}}}{-W} + \frac{J^{*2}}{-4W}, \; u = \frac{J^{*2}}{4W}$$

- Nodal metal is described by a **Hatsugai-Kohmoto model**.
- Non-Fermi liquid excitations.

$$\Sigma \sim \frac{u^2}{\omega}, Z \sim \omega^2$$

Σ pole continues into **Mott insulator**.

For $q_1 \neq q_2$, we find **charge fluctuations**:

$$\phi^\dagger_{\mathbf{q}_1,\bar{\sigma}}\phi^\dagger_{\mathbf{q}_1,\sigma}\phi_{\mathbf{q}_2,\sigma}\phi_{\mathbf{q}_2,\bar{\sigma}}$$

Might become dominant upon **doping**!

Baskaran 1991; Hatsugai and Kohmoto 1992; Phillips, Yeo, and Huang 2020.

Non-local nature of the pseudogap

- real-space correlations and entanglement undergo a crossover within the pseudogap from short-ranged to **long-ranged** behaviour
- This is further evidence of the **breakdown of local Kondo screening**, and resulting Landau quasiparticle excitations
- the Mott transition observed by us for the Hubbard-Heisenberg model on the square lattice lies well beyond the paradigm of **local quantum criticality**

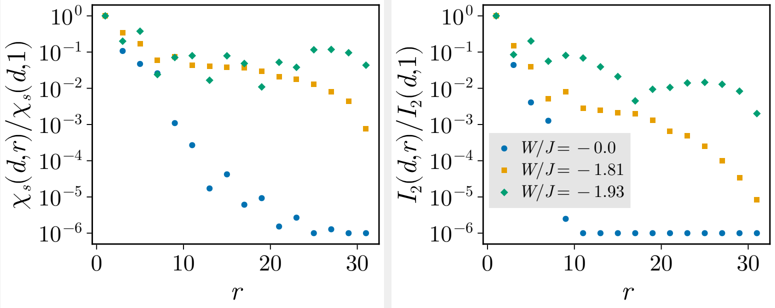

Conclusions: Main Takeaways

Realisation of **Mott's original vision** (1949) with deconfined holes & doubles

- new, (likely) universal phase of strongly interacting electronic quantum matter,
- noisy, incoherent environment for electron-like excitations,
- a long-ranged and multipartite entangled "quantum soup",
- scale invariant at Mott critical point & described by exactly solvable model (extremely rare in D>1!).

Fate at non-zero temperatures & doping?

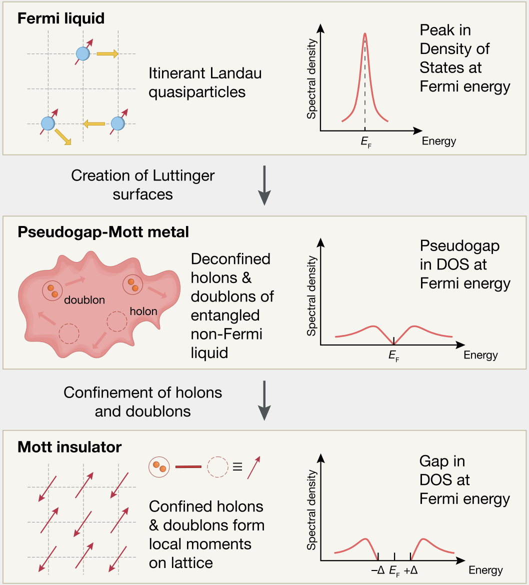

Brief Mentions of Other Projects

Kondo frustration via charge fluctuations: a route to Mott localisation
New J. Phys. 25 113011 (2023)
Precursor to the Mott metal work. Demonstrated how an extended Anderson impurity model captures the $d = \infty$ Mott MIT on the Bethe lattice.

Holographic entanglement renormalisation for fermionic quantum matter
J. Phys. A: Math. Theor. 57 275401 (2024)
Demonstration of the holographic principle by showing how entanglement renormalisation in a free fermion system leads to a holographic dimension.

Revealing the magnetic dimensional crossover in the Heisenberg ferromagnet CrSiTe3 through picosecond strain pulses
Phys. Rev. B 111, L140414 (2025)
Investigated the two-step magnetic dimensional crossover in CrSiTe3. We came up with a simple Ginzburg-Landau model of phonons interacting with the lattice spin fluctuations to explain the softening/gapping of various phonon modes.

Brief Mentions of Other Projects

Frustration shapes multi-channel Kondo physics: a star graph perspective
J. Phys.: Condens. Matter 35 315601 (2023)
We investigated the single-channel Kondo model and demonstrated the presence of two-particle correlations and entanglement within the Kondo cloud in the form of an effective Hamiltonian; we also calculated how they evolved during the high to low-temperature crossover.

Unveiling the Kondo cloud: Unitary RG study of the Kondo model
Phys. Rev. B 105, 085119 (2022)
Shed light on the role played by the ground state degeneracy in the non-Fermi liquid physics - how it leads to an orthogonality catastrophe in the low-energy excitations and how it modified the various correlations into anomalous forms.

Future Interests

Backup Slides

Tiled Entanglement

Concentration of S_{EE} and I_2 within the nodal region